Cellulose (2017) 24:1759–1773
DOI 10.1007/s10570-017-1220-2

ORIGINAL PAPER

Multi-layer nanopaper based composites

Andreas Mautner · Jessica Lucenius · Monika Österberg · Alexander Bismarck

Received: 13 July 2016 / Accepted: 13 February 2017 / Published online: 20 February 2017

Abstract Native cellulose nanofibrils (CNF) were prepared from bleached birch pulp without any chemical or enzymatic pretreatment. These CNF were modified by adsorption of a small amount of water-soluble polysaccharides and used to prepare nanopapers, which were processed into composites by lamination with an epoxy resin and subsequently cured. The results were compared to the properties of composites prepared using bacterial cellulose nanopapers, since bacterial cellulose constitutes highly pure and crystalline cellulose. It was found that both types of nanopapers significantly improved both the thermal stability and mechanical properties of the epoxy resin. As anticipated, addition of only 2 wt% of water-soluble polysaccharides efficiently hindered crack-propagation within the nanopaper and significantly improved the tensile strength and work of fracture compared to composites containing a conventional nanopaper reinforcement. The mechanical properties of the composites thus reflected the improvement of the nanopaper properties by the polysaccharides. Moreover, it was possible to predict the properties of the final composite from the mechanical performance of the nanopapers.

Keywords Nanocellulose · Bacterial cellulose · Epoxy resin · Nanocomposite

Andreas Mautner and Jessica Lucenius have contributed equally as first authors.

A. Mautner · A. Bismarck
Polymer and Composite Engineering (PaCE) Group, Faculty of Chemistry, Institute for Materials Chemistry and Research, University of Vienna, Vienna, Austria

J. Lucenius · M. Österberg
School of Chemical Technology, Department of Forest Products Technology, Aalto University, Espoo, Finland

A. Bismarck (✉)
Polymer and Composite Engineering (PaCE) Group, Department of Chemical Engineering, Imperial College London, London, UK
e-mail: alexander.bismarck@univie.ac.at
URL: http://mc.univie.ac.at

Introduction

During the last decades natural fiber composites have gained renewed attention due to environmental issues associated with conventional composites produced from synthetic materials (Moon et al. 2011; Blaker et al. 2014; Mariano et al. 2014). Even though progress was made in recycling of high performance composites, these types of materials still pose significant waste issues (Montrikittiphant et al. 2014; Pimenta and Pinho 2011). Thus, composites based on renewable resources, utilizing clean and cheap production routes have been proposed as an alternative (Lee et al. 2012c). Among the most promising approaches identified for the production of high performance

renewable composites was the use of cellulose nanofibrils as reinforcement for polymers (Lee et al. 2014a).

Recently, cellulose nanofibrils (CNF) with diameters at the nanoscale received much attention due to their outstanding chemical and mechanical properties (Chen et al. 2010; Lee et al. 2012a; Klemm et al. 2011). They were utilized for a wide range of applications (Klemm et al. 2011), such as membranes (Mautner et al. 2014, 2015), flame-retardant and fire-protection applications (Carosio et al. 2015, 2016; Liu and Berglund 2013) and in particular for the production of composites (Blaker et al. 2011; Lee et al. 2009, 2012b c, 2014b; Nogi and Yano 2008; Lee and Bismarck 2012; Eichhorn et al. 2010; Pommet et al. 2008; Wan et al. 2006). Accordingly, numerous approaches to utilize CNF in composites have been proposed and tested. One approach to utilize the potential of CNF was to directly reinforce a soft matrix with small amounts of CNF, which resulted in improved strength of the composites provided that the affinity between matrix and cellulose fibrils was high enough. Mikkonen et al. (2011) utilized 5–15 wt% of CNF to reinforce spruce O-acetyl galactoglucomannan films while Peng et al. (2011) and Hansen et al. (2012) reinforced xylan films. Additionally, chitosan based and thermoplastic starch composites were reinforced by CNF (Tomé et al. 2013): Addition of 10–20 wt% of CNF was sufficient to improve the thermal stability and mechanical properties of the composites, i.e. the Young's modulus and the tensile strength improved significantly at the expense of the ductility of the composite. To manufacture hierarchical composites, cellulose microfibers were combined with CNF (Lee et al. 2012a, 2014c), but also utilization of CNF as sole reinforcing agent was considered a possible track en route to high performance composites (Eichhorn et al. 2010).

The best results have been obtained using a biomimetic approach; introducing a very high loading of CNF in a small amount of a soft polymer. While the CNF matrix provides stiffness and strength, the role of the soft polymer is to dissipate energy and hinder crack propagation, thus improving toughness. This ultimately aims at exceeding the mechanical properties of the individual constituents of the composite. For example, a cationic block-co-polymer was combined with highly negatively charged CNF, resulting in synergistic effects (Wang et al. 2011; Sehaqui et al. 2013). Unfortunately, this led to the removal of water from the CNF gel due to ionic interactions between cationic polymer chains and anionic fibrils resulting in fibril aggregation. CNF aggregation easily leads to defects in the composite, therefore it is very important to control the interactions between the individual fibrils and avoid aggregation (Benítez et al. 2013). Thus, approaches utilizing non-ionic interaction between a polymer matrix and cellulose have been suggested, e.g. CNF were combined with poly(ethylene glycol) grafted carboxymethyl cellulose (Olszewska et al. 2013a, b). Furthermore, bacterial cellulose (BC) was combined with hydroxyethyl cellulose (Zhou et al. 2009). Within these systems, the contact points between fibrils during film formation were lubricated by the water-swollen polysaccharides, leading to the formation of strong films. Further aligning the fibrils did substantially improve the strength and stiffness of the composite in one direction (Sehaqui et al. 2012).

While there have been extensive efforts to prepare thin nanopapers and composites from CNF, there are only a few reports where these nanopapers have been used to prepare (nano)paper based laminated composites to utilize the CNF properties. This would be of outmost practical importance. The use of nanopapers as reinforcement for polymers was first demonstrated by Yano (Yano et al. 2005; Nakagaito and Yano 2005). Henriksson and Berglund (2007) later prepared nanopaper-composites with a water-soluble melamine–formaldehyde resin while Lee et al. (2012c), Ansari et al. (2014) and Aitomäki et al. (2016) manufactured epoxy composites by vacuum infusion and impregnation, respectively. However, as of yet, not much research has focused on the effect of the nanopaper properties on composite properties. We hypothesize that the properties of the nanopaper reinforcement strongly affect the properties of the composite in multi-layer laminates. It would be very desirable to have a process at hand in which the mechanical properties of final multi-layer composites were defined by the mechanical performance of the nanopaper base.

It was previously found that adding only 2 wt% of water-soluble polysaccharides to a suspension of CNF significantly improves the dry and wet strength of CNF nanopapers (Lucenius et al. 2014). In this study, we aimed to make use of this increased nanopaper strength for production of multi-layer, laminated paper

based composites with improved mechanical and thermal stability. Furthermore, it was our aim to demonstrate a process resulting in predictable nanocomposite properties. Nanocomposites were prepared by lamination of nanopapers. The production of these nanopaper laminates and their characterization are reported. Furthermore, composites based on bacterial cellulose (BC) nanopapers were produced as control and compared with the CNF nanopaper composites. The reasons behind the observed effects were discussed.

Experimental

Materials

Cellulose nanofibrils (CNF) were prepared by disintegration of unmodified never dried industrial bleached birch pulp. The pulp was passed six times through a high-pressure fluidizer (Microfluidics, M-110Y, Microfluidics Int. Co., Newton, USA) following a procedure described previously (Österberg et al. 2013). The CNF had diameters ranging between 5 and 100 nm but the majority of the fibrils were in the range of 5–20 nm with a few larger fibril bundles being present. The length of the fibrils was a few micrometers. No loss of mass was observed during the fibrillation process. Commercially available bacterial cellulose was kindly supplied by fzmb GmbH (Bad Langensalza, Germany) in the form of wet pellicles containing 92 wt% water. The diameter of BC was found to be approximately 50 nm with fibril lengths of up to several micrometers (Lee and Bismarck 2012).

Two types of water-soluble polysaccharides (WSPS) were introduced into the CNF network. Commercial guar gum galactomannan (GG, $M_w > 1000$ kDa) from Sigma Aldrich (Lot#041 M 0058 V, Pcode 10011170894) was used after enzymatic modification. Spruce galactoglucomannan (GGM, Picea abies, M_w 20–60 kDa) was extracted from the process water of a Finnish pulp mill in an industrial-scale isolation trial after ethanol precipitation (Xu et al. 2008). Enzymes were used to hydrolyze and oxidize GG. Endo-1,4-β-mannanase (Lot 00803, from Aspergillus niger, EC number 3.2.1.78, 42 U mg^{-1}) was purchased from Megazyme (Wicklow, Ireland), galactose oxidase (GO, G7400, 3685 U g^{-1}, EC 1.1.3.9), catalase (from bovine liver, C30, 22,000 U mg^{-1}) and horseradish peroxidase (HRP, P8250, type II, 181 U mg^{-1}) from Sigma-Aldrich.

Epoxy resin (Araldite LY 556) and amine hardener (XB 3473) were purchased from Mouldlife (Suffolk, UK). The water used for all experiments was deionized and further purified in a UV unit (Synergy Millipore, Molsheim, France). $NaNO_3$ and $NaBD_4$ were purchased from Aldrich and used as received.

Methods for CNF modification, nanopaper and composites production and testing

Hydrolysis and oxidation of GG

Endo-1,4-β-mannanase was used to partially hydrolyze GG. GG was dissolved in deionized water to produce a 1.0% (w/v) solution, the enzyme added and the solution incubated at 40 °C in a water bath for 4 h. In order to deactivate the enzyme it was heated to 100 °C for 10 min. The samples were centrifuged at 5000 rpm and the supernatant was collected and freeze-dried.

Hydrolyzed GG was enzymatically oxidized (OGG) whereby the dosage of the enzymes was based on the amount of galactose present in the GG sample: 1.50 units (U) of GO, 150 U of catalase and 0.9 U of HRP per mg of galactose (Lucenius et al. 2014; Parikka et al. 2010). 1% (w/v) solutions of GG were stirred in the presence of the enzymes at +4 °C for 72 h. Afterwards the sample was heated to 90 °C while mixing in order to inactivate the enzymes.

Determination of the molecular weight and the degree of oxidation of GG

The molecular weight (M_w) of GG hydrolyzed with mannanase was determined using size exclusion chromatography (SEC). M_w was calculated using a dn/dc value of 0.15 mL g^{-1}. The hydrolyzed GG was dissolved in 0.1 M $NaNO_3$ by stirring for 7 d and filtered through a 0.45 µm filter. The method is described in detail by Parikka et al. (2010).

Gas chromatography mass spectrometry (GC–MS) was used to determine the degree of oxidation (DO). Briefly, the samples (1 mg of polysaccharide) were deuterium labelled with $NaBD_4$, precipitated and acid methanolyzed. GO was used to selectively oxidize the galactosyl units of GG. The degree of oxidation was calculated as described in literature (Parikka et al. 2010).

Nanopaper preparation

To avoid nanofibril aggregation, the CNF suspension was diluted to 0.8 wt% (105 mL, corresponding to a dry mass of 0.84 g) and mixed overnight using a magnetic stirrer. To this suspension, 2 wt% (based on CNF dry content) of water soluble polysaccharides OGG or GGM, respectively, were added and further stirred for 24 h to ensure homogeneity (Lucenius et al. 2014). Sequential filtering and pressing (Österberg et al. 2013) was used to prepare the CNF-WSPS nanopapers. CNF-nanopapers with grammages of 60 g m^{-2} were prepared.

Nanopapers from BC were prepared as previously reported (Mautner et al. 2015; Lee et al. 2012c). Briefly, the BC pellicles were first cut into small pieces (with a length of approximately 5–10 mm) and blended (Breville VBL065-01, Oldham, UK) for 2 min at a consistency of 0.2 wt% in deionized water to produce a homogeneous suspension of BC-in-water. These suspensions were then vacuum-filtered onto a cellulose filter paper (VWR 413, 5–13 μm pore size, Lutterworth, UK). The wet filter cake was wet-pressed under a weight of 10 kg between blotting papers (3MM Chr VWR, Lutterworth, UK) for 5 min to further remove excess water. These wet filter cakes were then consolidated and dried in a hot-press (25-12-2H, Carver Inc., Wabash, USA) under a compression weight of 1 t for 1 h at 120 °C by sandwiching the wet filter cakes between fresh blotting papers and metal plates. BC-nanopapers with grammages of 50 g m^{-2} were prepared.

Preparation of nanopaper based composites

Composites were manufactured by laminating nanopapers with a two-component epoxy resin. Commercially available epoxy resin Araldite LY 556 plus 23 phr amine hardener XB 3473 were mixed and degassed under vacuum at 80 °C for 10 min. Two nanopapers (diameter 120 mm) were laminated using a K Printing Proofer (RK PrintCoat Instruments Ltd, Hertfordshire, UK) at room temperature by applying a 50 μm layer of epoxy resin in between two nanopapers. After lamination the nanopaper-epoxy laminate was sandwiched between two Teflon films in a custom-made mold and placed into a hot-press. The hot-press was heated to 120 °C. When reaching this temperature the sandwich was pressed at 2 t for 2 h. Afterwards the temperature was increased to 180 °C for an additional 2 h. The composite was de-molded after cooling under pressure to room temperature. From the final composites, strips with dimensions of 40 × 5 mm^2 were cut with a lab paper cutter.

Mechanical properties of the composites

Dynamic Mechanical Analysis of the composites was performed with a G2 RSA (TA Instruments, Eschborn, Germany) in three point bending mode. Specimens sized 40 × 5 mm^2 were cut from the composites and tested between −50 and 250 °C at 3 °C min^{-1} and a frequency of 1 Hz, an applied strain of 0.05% and a span distance of 25 mm.

Tensile properties of the composites were determined on at least five specimens for each material at 25 °C and 50% RH using a 5969 Dual Column Universal Testing System (Instron, Darmstadt, Germany) equipped with a 1 kN load cell. The thickness of the composites was measured for each specimen before each test at ten different spots using a digital micrometer (705–1229, RS components, Corby, UK). The gauge length was 20 mm and the testing velocity 0.5 mm min^{-1}.

Morphology of the composites

The morphology of CNF-GGM composite films was studied using a high resolution scanning electron microscope (JEOL JSM-7500FA, Tokyo, Japan) in the Nanomicroscopy center at Aalto University and a Benchtop SEM (Jeol JCM-6000 Neoscope) in Vienna. The samples were freeze-dried in liquid nitrogen and fractured in half using tweezers while in the liquid nitrogen bath. Dust and loose particles were removed from the samples by blowing with nitrogen. A thin layer of gold/palladium (Emitech K100, Aalto) or gold only (JEOL JFC-1200 Fine Coater, Vienna) was sputtered on the sample surface to ensure sufficient electrical conductivity.

Thermal degradation behavior of nanopapers and composites

The thermal degradation behavior of nanopapers and composites in nitrogen and air, respectively, was investigated using a high resolution modulated TGA (Discovery TGA, TA Instruments, Eschborn,

Germany). A sample size of approximately 5 mg was used. The samples were heated from 30 to 650 °C at a heating rate of 10 °C min^{-1} and a gas flow rate of 25 mL min^{-1}. The onset of degradation was computed to be the temperature at which the mass loss rate was exceeding 0.2% per °C.

Results and discussion

A small amount of water-soluble polysaccharides (WSPS) as low as 2 wt% was introduced into the fibril network of non-pretreated CNF nanopapers and their influence on the thermal and mechanical performance of laminated nanopaper-epoxy composites evaluated. The polysaccharides studied were the mannans GGM and GG, which contain ca. 10 and 40% terminal α-D-galactosyl residues, respectively. These residues are directly attached to the C-6 of the mannosyl units of the backbone (Wielinga 2009). GG was hydrolyzed to reduce the molecular weight and enzymatically oxidized at the C-6 position of the mannosyl units to improve the mechanical performance (Lucenius et al. 2014). The effect of the polysaccharides used to modify the CNF and the differences between BC, constituting highly pure and crystalline cellulose, and modified CNF on the nanopaper and composite properties are discussed.

Structure and properties of the WSPS and nanopapers

WSPS GGM was utilized in its unmodified state, whereas low molecular weight GG was prepared by partial hydrolysis with β-mannanase (Lucenius et al. 2014). The M_w of the hydrolyzed GG, as determined by size exclusion chromatography, was approximately 30 kDa as compared to 1000 kDa before hydrolysis (Wielinga 2009).

Hydrolyzed GG was subsequently oxidized (Scheme 1) with galactose oxidase (GO), catalase and horseradish peroxidase (HRP) (Parikka et al. 2010). The degree of oxidation (DO) of oxidized galactosyls in OGG was 50% (OGG-50) and 80% (OGG-80), respectively. The total amount of oxidized carbohydrates in hydrolyzed GG was 20 and 31%, respectively, and the total relative amount of oxidized galactosyls in the final modified nanopaper was found to be 0.375 and 0.60% of total carbohydrates, respectively. The backbone of GG remained unmodified due to the selective oxidation of the galactosyls, facilitating good compatibility with cellulose. Furthermore, the viscosity of the OGG solutions was low at both degrees of oxidation, enabling good mixing with the CNF suspension. Extensive mixing was used to ensure homogeneous distribution of WSPS in the CNF suspension. Nanopapers with grammages of 60 g m^{-2} were produced from CNF with and without 2 wt% of GGM or OGG, respectively, and from BC (50 g m^{-2}) using a simple papermaking process (Mautner et al. 2015). The final thickness of the nanopapers was 60 ± 5 μm for (modified) CNF and 50 ± 5 μm for BC nanopapers.

The tensile strength (88 MPa) of unmodified CNF nanopapers improved by more than 50% by CNF modification with oxidized GG (135 MPa) or GGM (141 MPa). This took place at the expense of stiffness, as shown by the slight decrease of the modulus from 9 GPa for unmodified CNF to 7.9 GPa for oxidized GG. For GGM (8.7 GPa) on the other hand no significant modulus decrease was observed. This was expected for WSPS modified nanopapers, in which WSPS act as plasticizer between stiff CNF, enhancing the ductility of the nanopaper in accordance with previous results (Lucenius et al. 2014; Olszewska et al. 2013b). During film formation from aqueous suspensions, the WSPS form a water-swollen dissipative layer on the CNF surface (Lozhechnikova et al. 2014; Eronen et al. 2011), thus enhancing the dispersibility of CNF. This is crucial to avoid CNF aggregation and defects in the final nanopaper resulting in improved mechanical properties. For BC nanopapers, a Young's modulus of 8.3 GPa and a tensile strength of 144 MPa were measured, which are values typically found for BC nanopapers prepared without prior removal of fibril aggregates (Lee et al. 2012c).

Multi-layer epoxy-nanopaper composites

Multi-layer composites were produced by a laminating technique impregnating (modified) CNF as well as BC nanopapers with a two-component epoxy resin. Resulting CNF composites had thicknesses around 100 μm and a fibril content of around 80 vol%. For BC composites the thickness was around 90 μm and the fibril content around 80 vol%. The reduced thickness of the composites was explained by further compaction of the nanopapers in the compression step

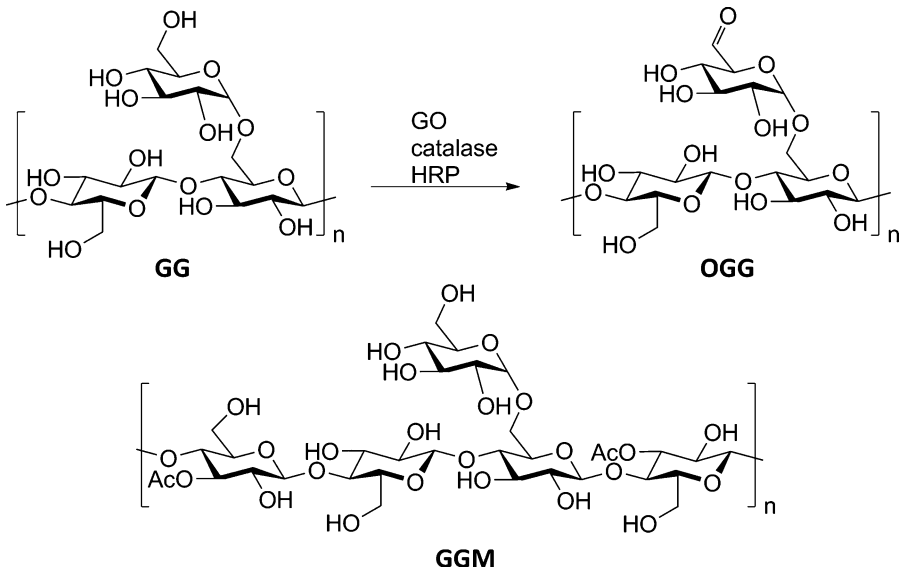

Scheme 1 Structures and modification of used polysaccharides. *(O)GG* (oxidized) guar gum galactomannan, *GGM* galactoglucomannan

during composite production. The mechanical performance of laminated nanopaper-epoxy composites as a function of temperature was evaluated by means of DMTA in three point bending mode.

The nanopaper-epoxy composites, as exemplarily shown for a BC and a CNF-OGG 80 composite in Fig. 1, exhibited the typical behavior of stiff, high glass transition thermosets; the modulus decreases slightly with increasing temperature and tanδ stays constant at a very small value. The CNF nanopaper based composites exhibited slightly lower modulus compared to BC nanopaper based composites with a stronger decrease at elevated temperatures. It was shown that these composites can be used up to almost their degradation temperature (see below) without passing the glass transition region of the epoxy matrix. The pure, cured epoxy resin follows the same principal trend up to 170 °C, but has a significantly lower storage modulus. The storage modulus at 20 °C was 2.54 GPa compared to around 17 GPa for nanopaper composites. However, at 170 °C the storage modulus of the epoxy resin decreased significantly, while tanδ increased indicating the onset of the glass transition. The glass transition temperature (T_g), taken as the maximum of tanδ, was 196 °C. Thus the introduction of nanopapers into an epoxy resin matrix not only improved mechanical properties, but also increased the application temperature range significantly. No T_g of neither BC nor CNF composites could be detected up to the onset of the degradation temperature around

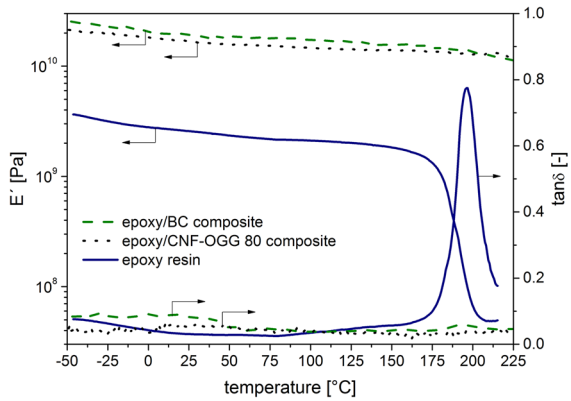

Fig. 1 Storage modulus E′ and loss factor tanδ as function of temperature for cured epoxy resin films (*blue full line*), an epoxy-CNF-OGG 80 composite (*black dotted line*) and an epoxy-BC composite (*green dashed line*). (Colur figure online)

250 °C, at which the composites still had a storage modulus of around 10 GPa.

The storage modulus at 20 °C was used to assess the influence of different WSPS on the mechanical performance of laminated nanocomposites (Table 1). As already shown for (modified) nanopapers (Lucenius et al. 2014), also the modulus of the composites depended on the type of polysaccharide introduced into the nanopaper. Composites containing an unmodified CNF nanopaper reinforcement had a storage modulus of 20 GPa, whereas for composites containing WSPS modified CNF nanopapers it was slightly lower, indicating the capacity of WSPS to act as

Table 1 Results of DMTA and tensile tests of BC and (modified) CNF-epoxy composites: Storage modulus at 20 °C, Young's modulus, tensile strength, strain at break and work of fracture

Sample	Storage modulus (GPa)	Tensile strength (MPa)	Young's modulus (GPa)	Strain at break (%)	Work of fracture (MJ m^{-3})
Epoxy	2.54 ± 0.05	36.1 ± 1.7	1.6 ± 0.1	4.16 ± 0.39	0.87 ± 0.12
Epoxy + CNF	20.0 ± 2.4	84.6 ± 4.3	12.2 ± 0.5	0.88 ± 0.09	0.34 ± 0.03
Epoxy + CNF/OGG-50	17.2 ± 1.0	89.8 ± 3.2	12.2 ± 0.5	0.78 ± 0.09	0.35 ± 0.03
Epoxy + CNF/OGG-80	17.4 ± 0.6	107.1 ± 6.1	10.7 ± 0.4	1.23 ± 0.17	0.63 ± 0.09
Epoxy + CNF/GGM	17.4 ± 0.2	116.8 ± 4.5	12.0 ± 1.0	1.17 ± 0.12	0.69 ± 0.11
Epoxy + BC	18.5 ± 0.5	150.8 ± 9.3	9.0 ± 0.1	2.76 ± 0.29	2.68 ± 0.41

lubricant. For BC nanopapers, a storage modulus of 18.5 GPa was measured, thus being in between the CNF nanopapers with and without WSPS modification.

In addition to DMTA, tensile tests were performed to determine the ultimate tensile strength, tensile modulus, strain at break and work of fracture. The work of fracture can be considered to be an indicator of the toughness of the composites. Representative stress–strain-curves from tensile tests of (modified) CNF nanopaper based composites are shown in Fig. 2 and all results are collected in Table 1.

The ultimate tensile strength was determined to be 85 MPa for the epoxy composite reinforced by two pure CNF nanopaper layers, compared to 36 MPa for the pure epoxy resin. Addition of OGG with a DO of 50% to the CNF did not significantly influence the tensile strength, while a DO of 80% for OGG led to a significantly improved tensile strength of the nanocomposites. This dependency on the DO was as to be expected (Lucenius et al. 2014) and showed that only a sufficiently high DO leads to an improved tensile strength. This can be explained by the low total amount of oxidized galactosyls in the composite, whereby oxidized galactosyls create hemiacetal crosslinks between hydroxyl and aldehyde groups of CNF and WSPS, which is likely to be the reason for stronger nanopapers as intermolecular crosslinks formed between fibrils. The higher the degree of oxidation was, the higher the tensile strength of CNF nanopapers (Lucenius et al. 2014) and correspondingly also of the composites. The effect was more pronounced for composites containing OGG-80 modified nanopaper reinforcements. Crosslinking has previously been shown to be beneficial for CNF composites (Lee et al. 2014a). Here it was shown that it is possible to control the mechanical properties of CNF

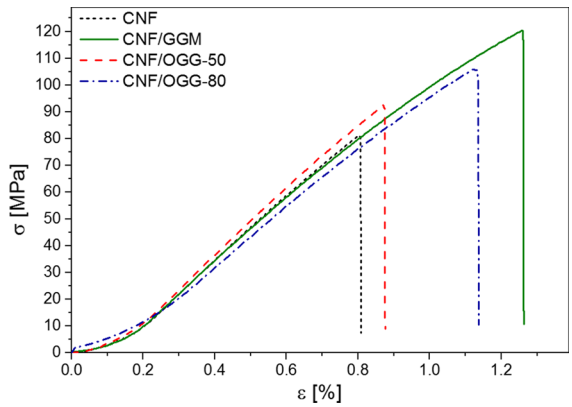

Fig. 2 Representative stress–strain curves for composites with pure CNF (*black dotted line*), CNF/OGG-50 (*red dashed line*), CNF/OGG-80 (*blue dash-dotted line*) and CNF/GGM (*green full line*) reinforcement. The setting behavior (up to 0.2% strain) of the specimens were due to handling difficulties owing to the thin laminates. (Colur figure online)

nanocomposites by controlling the composition and thus mechanical properties of nanopapers.

As anticipated, the highest tensile strength among CNF composites was observed when using CNF/GGM nanopaper reinforcements. Accordingly, just as for the pure nanopapers, GGM exhibited the highest reinforcing ability also within composites. This means that 80% of the original strength of the nanopapers was retained in the composites, which can be expected considering that a fibril fraction of 80 vol% was used to reinforce the resin. Thus the hypothesis of producing better performance cellulose nanocomposites when using better nanopapers was proven to be correct. The introduction of only 2 wt% WSPS into a CNF nanopaper network resulted in nanopapers with improved mechanical properties and the preparation of high loading fraction CNF nanocomposites from these nanopapers led to increased tensile strength of

the nanocomposites. Furthermore, the extent of the improvement could be estimated based on the mechanical properties of the nanopapers. The increase of the strength went hand in hand with a reduction of the modulus, as was already demonstrated in three point bending mode by DMTA (see above). While there was no detectable influence of the low DO OGG-50 on the composite modulus, for the higher DO OGG-80 grade a slight reduction compared to pure CNF and CNF/OGG-50 reinforced composites was observed. For GGM a small reduction of the tensile modulus was found. Modified CNF composites exhibited both enhanced Young's modulus and tensile strength compared to a previous study (Lee et al. 2012c) utilizing CNF nanopapers that were vacuum-infused with a brittle epoxy resin. This improvement was enabled by modification of the CNF by adsorbed WSPS. The introduction of WSPS seems to affect crack propagation in the nanopapers and thus also in the composites. The higher modulus compared to the nanopapers can be explained by further compaction of the laminates and accordingly the nanopapers during composite manufacturing.

The strain at break and work of fracture were determined for the composites from stress–strain-curves. For the nanopaper reinforcement modified with low DO OGG-50 grade again no detectable difference was found compared to pure CNF, which was explained by a too low DO leading to an insufficient amount of hemiacetal bonds forming within the nanopapers. For OGG-80 modified nanopaper reinforced composites the strain at break was significantly higher, which, in conjunction with higher tensile strength, resulted in significantly increased work of fracture. The same was found for GGM modified CNF nanopaper based composites.

Bacterial cellulose nanopapers were also tested for their reinforcing ability in composites. BC is purer than wood derived CNF due to the absence of hemicelluloses and lignin (Klemm et al. 2011). Moreover, long, entangled and homogeneous fibrils are responsible for good mechanical performance (Paakko et al. 2008; Klemm et al. 2011; Lee et al. 2014b). Therefore a higher reinforcing ability compared to CNF can be anticipated. This assumption was proven correct; the tensile strength of the BC nanopaper composites was the highest within this study with 151 MPa. However, BC composites had a lower tensile modulus compared to CNF nanopaper based composites, due to lower packing efficiency caused by thicker BC fibrils. Furthermore, hemicelluloses present in CNF nanopapers, which are absent in BC, enable a better stress transfer between CNF fibrils (Iwamoto et al. 2008; Lee et al. 2012c; Gröndahl et al. 2004). This was in good agreement with the DMTA results and literature (Lee et al. 2012c). BC composites even had higher tensile strength and modulus compared to pure BC nanopapers. This can be explained by further compaction of the nanopapers during composite manufacturing; i.e. the composites are thinner than 2 nanopaper layers. Moreover, a very high strain at break and thus work of fracture was measured for BC composites. The higher strain to break for BC composites can be explained by fewer physical crosslinking points between the BC nanofibrils, allowing for realignment of the fibrils during tensile loading (Lee et al. 2012c) and the higher length of BC fibrils compared to CNF. The reorientation of the fibrils even within the composites was still possible since the resin did not fully impregnate the BC nanopapers because of the small pore dimensions and low nanopaper porosity of 33%.

The fracture surfaces of the composites were inspected by SEM. In Fig. 3, the fracture surfaces of composites made from CNF, CNF/GGM, CNF/OGG-50, CNF/OGG-80 and BC nanopapers are shown.

The layered structure of the nanopapers can be easily seen. In the center of the composites, a pure, 5–10 μm thick epoxy resin phase can be observed. The resin spreads into both nanopapers, thus ensuring good adhesion between nanopapers and resin, as well as holding the nanopapers together. However, the larger part of the nanopapers was not impregnated, thus allowing for realignment of the fibrils within the nanopapers. This is particularly true for the nanopapers containing WSPS, in which those polysaccharides act as lubricant in between the nanocellulose fibrils.

In the review by Lee et al. (2014b) poly-L-lactic acid (PLLA) was used as a benchmark because it is the best performing commercially available renewable bulk polymer. Compared to the PLLA standard, having a tensile modulus of 4 GPa and tensile strength 63 MPa, all the reinforced samples studied here well exceeded the mechanical properties of PLLA. If compared to other BC or CNF reinforced composites we note that especially the Young's modulus obtained for the GGM modified CNF nanopaper laminates exceeded most of the previously reported results, but

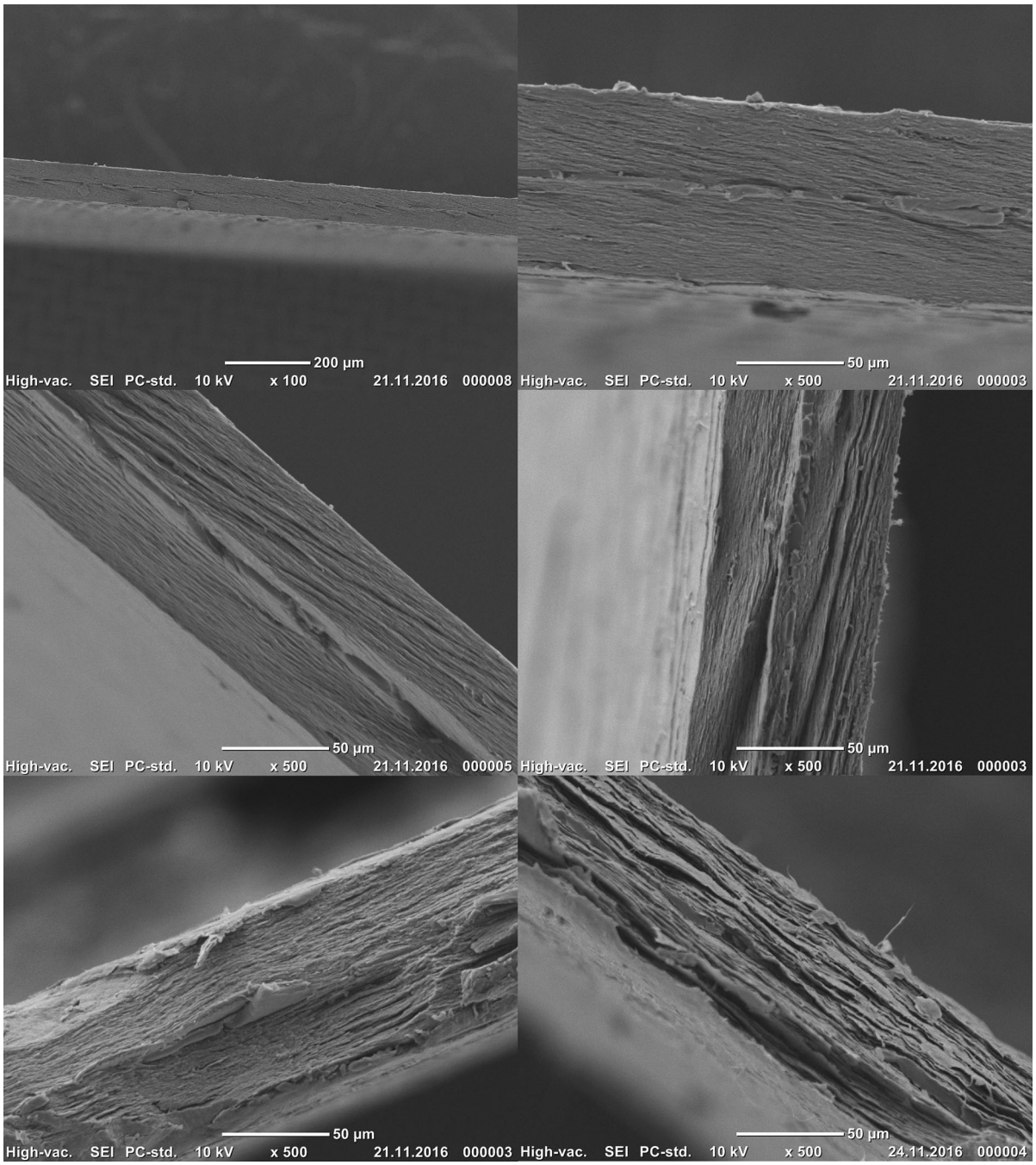

Fig. 3 SEM images (magnification: ×100 or ×500) of the fracture site of composites made from CNF (*top*, *left* ×100, *right*: ×500), CNF/GGM (*centre left* ×500), CNF/OGG-50 (*centre right* ×500), CNF/OGG-80 (*bottom left* ×500) and BC (*bottom right* ×500) nanopapers

the tensile strength was average. Other groups reported much higher values (Ansari et al. 2014; Henriksson et al. 2008; Sehaqui et al. 2010; Zhou et al. 2009), but since these have been obtained for thin nanopapers of chemically pre-treated CNF, they are not fully comparable to the results presented here. The nanopaper properties determine the properties of the final nanopaper based multi-layer composites,

allowing predicting the composites properties. It was found that addition of only 2 wt% of GGM for the preparation of CNF nanopaper resulted in doubling the work of fracture of the final composite. This result was obtained without any chemical pretreatment or synthetic polymers. Since the extraction of GGM from wood is scalable (Leppänen et al. 2011) this result is quite interesting. To produce even higher strength, co-polymers with grafted soft chains like CMC-g-PEG could be used, but that would at the same time increase the complexity of the system. It is further noteworthy that the nanopapers used also significantly improved the thermal stability of the epoxy composites.

Thermal behavior of nanopapers and nanopaper composites

The thermal degradation behavior of BC and CNF nanopapers alone was tested in both nitrogen (Fig. 4, left) and air (Fig. 4, right) atmosphere. A one-step degradation regime was observed for all types of nanopapers in inert atmosphere. During the initial testing phase between 30 and 150 °C, no significant difference was found for the different CNF nanopapers. Around 5% of moisture was removed for (modified) CNF nanopapers and the onset of the thermal degradation took place at around 275–280 °C. This degradation step was attributed to cleavage of glycosidic linkages of cellulose (USDA 1970). A smaller amount of moisture (2%) was removed from BC and the onset of the first degradation step occurred at 320 °C. This difference can be explained by a higher degree of crystallinity of BC (72 ± 1%) compared to CNF (60 ± 5%) (Österberg et al. 2013), which is due to the absence of residues of lignin and hemicelluloses (Lee et al. 2012c). A char residue at 600 °C of 12 and 13% was found for OGG-50 and OGG-80 modified CNF, respectively. For GGM modified CNF it was 16% and BC and unmodified CNF had a char residue of 17%.

In air atmosphere again around 5 and 2%, respectively, of moisture was removed between 30 and 150 °C for CNF and BC nanopapers, respectively. The first degradation step, attributed to the degradation of low-molecular weight glycosidic compounds (Cheng et al. 2009; Seifert et al. 2004), occurred around 250 °C for all the CNF nanopapers tested. For BC this temperature was higher (300 °C), similar to results reported in literature (Lee et al. 2012c). The second degradation step, attributed to the degradation of pyran structures, started for all types of CNF and BC nanopapers around 450 °C. Only minor deviations were found for modified CNF nanopapers; all modified nanopapers were completely degraded at 500 °C.

The thermal decomposition of composites is shown in Fig. 5. Similar to the pure nanopapers, a one-step degradation regime was observed for all types of composites in inert atmosphere (Fig. 5, left). This demonstrated that the overall thermal behavior was mainly governed by the nanopapers, which constitute

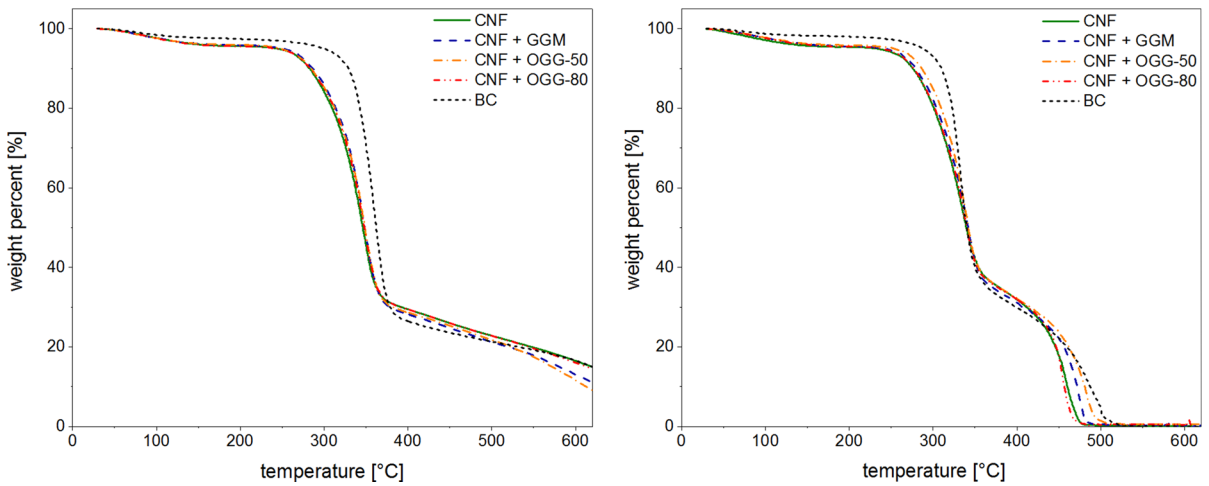

Fig. 4 TGA under nitrogen (*left*) and air (*right*) of CNF and BC nanopapers. CNF (*green full line*), CNF + GGM (*blue dashed line*), CNF + OGG-50 (*orange dash-dotted line*), CNF + OGG-80 (*red dash-double dotted line*) and BC (*black narrow dashed line*). (Colur figure online)

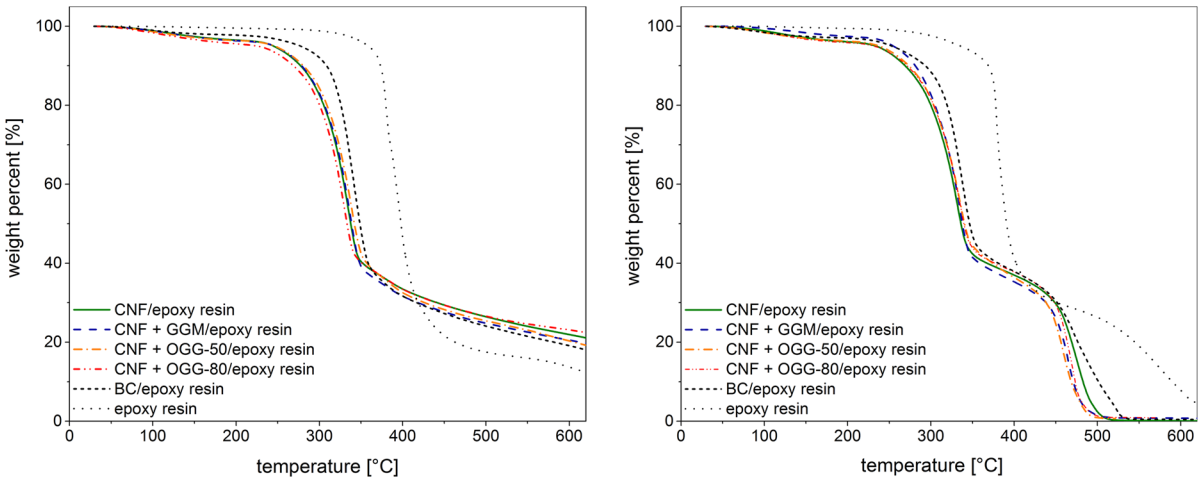

Fig. 5 TGA under nitrogen (*left*) and air (*right*) of CNF and BC-epoxy composites. CNF (*green full line*), CNF + GGM (*blue broad dashed line*), CNF + OGG-50 (*orange dash-dotted line*), CNF + OGG-80 (*red dash-double dotted line*), BC (*black narrow dashed line*) and epoxy resin (*black dotted line*). (Colur figure online)

the majority of the composites. However, during the initial degradation phase between 30 and 150 °C, only around 3% (compared to 5% for the CNF nanopapers) of moisture was removed for CNF composites. This was attributed to the increased overall hydrophobicity caused by the epoxy matrix. For BC composites this value (2%) was similar to the pure BC nanopaper. The onset of thermal degradation of CNF composites occurred at around 270 °C, comparable to the CNF nanopapers. For BC composites, the degradation commenced at 300 °C, which was slightly lower than for pure BC nanopapers. Final degradation was found to be somewhat different for the different sets of polysaccharide phases within the CNF nanopaper. A char residue at 600 °C of 19–22% was found for the various types of composites, thus being slightly higher than for the pure nanopapers and the epoxy resin alone.

In air atmosphere (Fig. 5, right), regarding removal of moisture, the same tendencies for differences between nanopapers and composites were found as in nitrogen. The first degradation step occurred at 270 °C (compared to 250 °C for CNF nanopapers), demonstrating the influence of the protecting epoxy matrix. Between (modified) CNF samples, no obvious difference was observed. For BC composites the onset temperatures of the first degradation step occurred at 293 °C, which was similar to pure BC nanopapers. Also for the onset of the second degradation step around 430 °C, hardly any deviations were found for the composites containing modified CNF nanopapers. For BC composites the onset of the second degradation step occurred at 450 °C, similar to those of the pure nanopapers and higher compared to CNF composites, which again was ascribed to the higher degree of crystallinity of BC. All the composites were completely degraded around 500 °C. The cured epoxy resin starts decomposing at 350 °C and was completely degraded at 650 °C.

In Fig. 6, the degradation of composites containing GGM modified CNF and BC, respectively, in inert atmosphere is contrasted to the degradation of the corresponding nanopapers. Furthermore, a theoretical degradation graph is displayed, constructed from the degradation of the epoxy resin and the nanopapers, assuming a resin content of 20%. Only minor differences between theory and experiment can be observed. The composites apparently start to degrade at slightly lower temperatures compared to the nanopaper, whereas a small increase would be theoretically expected. This might be due to thermal damage the nanopaper experiences during the composite production at 180 °C. Furthermore, a higher than expected amount of char residue was found. This can be explained by mutual protection of both nanopaper and epoxy resin.

Figure 7 shows the degradation behavior of the pure and modified nanopapers and composites containing GGM modified CNF and BC nanopapers in air together with the theoretical degradation graph constructed from the degradation of the epoxy resin and

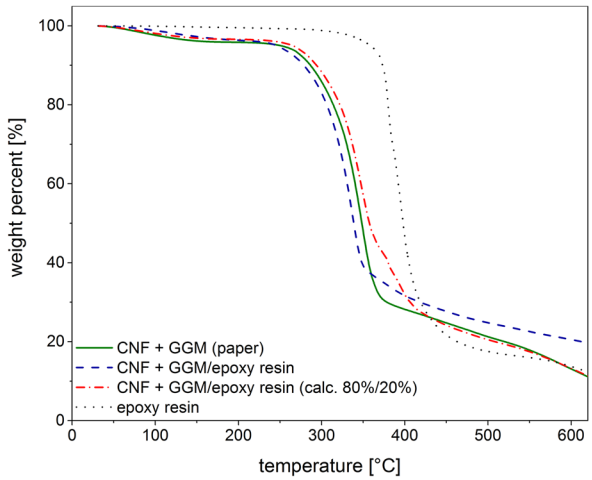

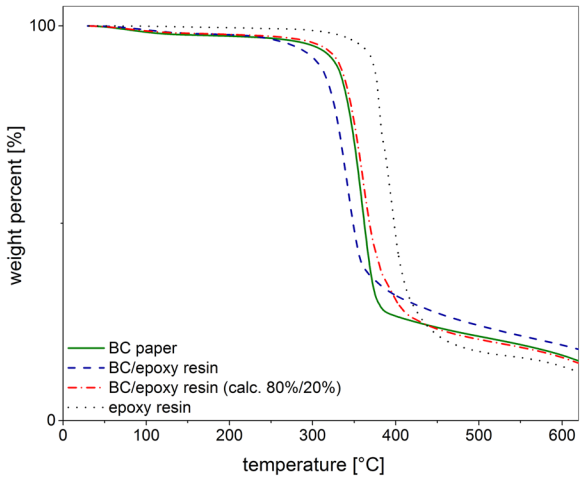

Fig. 6 TGA under nitrogen of CNF + GGM (*left*) and BC (*right*) epoxy composites and nanopapers. Nanopaper (*green full line*), composite (*blue broad dashed line*), theoretical degradation of a composite assuming 20% resin content (*red dash-dotted line*) and epoxy resin (*black dotted line*). (Colur figure online)

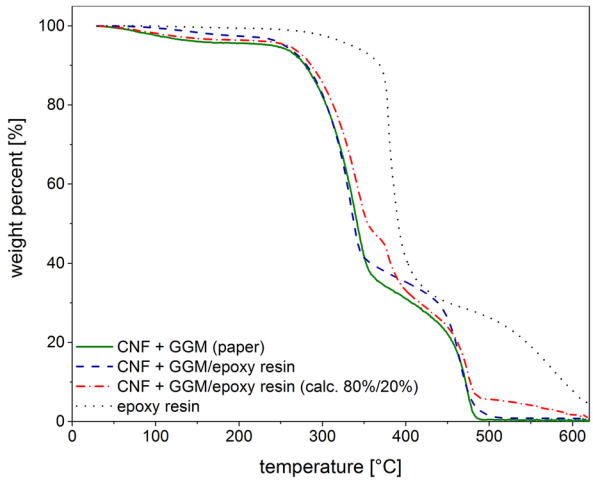

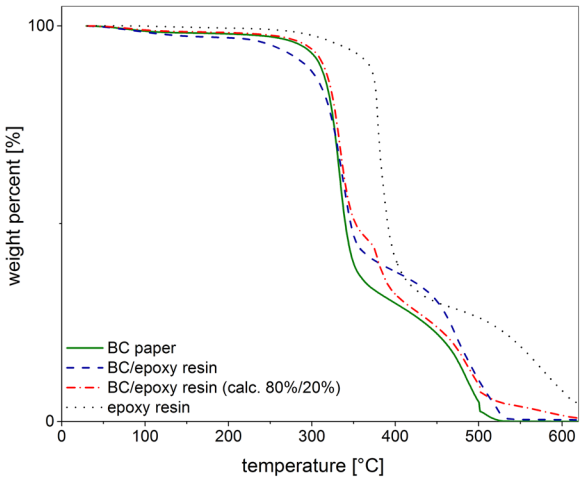

Fig. 7 TGA under air of CNF + GGM (*left*) and BC (*right*) epoxy composites and nanopapers. Nanopaper (*green full line*), composite (*blue broad dashed line*), theoretical degradation of a composite assuming 20% resin content (*red dash-dotted line*) and epoxy resin (*black dotted line*). (Colur figure online)

the nanopapers assuming a resin content of 20%. In air the differences observed were even smaller as in nitrogen. Just as under inert atmosphere, the first degradation step starts at slightly lower temperatures whereas for the second degradation step hardly any difference was found at all.

Conclusions

Nanopapers prepared from non-pretreated CNF and water-soluble polysaccharide modified CNF were used as 2D reinforcement for epoxy resins, utilizing an easy process allowing for the preparation of multi-layer laminates with predictable properties. The CNF nanocomposites were produced by wet lamination and compared to BC nanopaper composites. Both CNF and BC nanopapers were successfully processed into multi-layer composites by lamination with an epoxy resin followed by curing in a hot-press. Significant improvements in both mechanical properties and application temperature were achieved. The mechanical properties of the paper based composites are determined by the properties of CNF nanopapers.

These improvements could be estimated based on the mechanical properties of the nanopapers and epoxy resin matrix. An addition of only 2 wt% of galactoglucomannan to CNF resulted in significantly improved tensile strength (50%) of the nanopaper, which in turn resulted in a 40% increase of the strength of the corresponding laminated epoxy composite containing 80 vol% CNF. Furthermore, the strain at break and work of fracture also improved. This was explained by the lubricating effect of the WSPS affecting crack propagation in the nanopaper. BC nanopaper composites exhibited even higher tensile properties as compared to the modified CNF nanopaper reinforced composites, which was explained by its higher degree of crystallinity. Moreover, it was found that the WSPS hardly affected the thermal degradation behavior of the CNF nanopapers and the thermal stability of the nanocomposites was mainly governed by the thermal behavior of the CNF nanopapers as they made up around 80 vol% of the composites.

Acknowledgments Open access funding provided by University of Vienna. Financial support by the Academy of Finland, Project 278279, as well as by the University of Vienna is greatly acknowledged. J.L. thanks the Nanomicroscopy Center at Aalto University for the possibility to conduct high resolution scanning electron microscopy and Juuso Korhonen for his assistance in setting up the microscope.

References

Aitomäki Y, Moreno-Rodriguez S, Lundström TS, Oksman K (2016) Vacuum infusion of cellulose nanofibre network composites: influence of porosity on permeability and impregnation. Mater Des 95:204–211

Ansari F, Galland S, Johansson M, Plummer CJG, Berglund LA (2014) Cellulose nanofiber network for moisture stable, strong and ductile biocomposites and increased epoxy curing rate. Compos Part A Appl Sci 63:35–44

Benítez AJ, Torres-Rendon J, Poutanen M, Walther A (2013) Humidity and multiscale structure govern mechanical properties and deformation modes in films of native cellulose nanofibrils. Biomacromolecules 14:4497–4506

Blaker JJ, Lee K-Y, Bismarck A (2011) Hierarchical composites made entirely from renewable resources. J Biobased Mater Bioenergy 5:1–16

Blaker JJ, Lee K-Y, Walters M, Drouet M, Bismarck A (2014) Aligned unidirectional PLA/bacterial cellulose nanocomposite fibre reinforced PDLLA composites. React Funct Polym 85:185–192

Carosio F, Kochumalayil J, Cuttica F, Camino G, Berglund L (2015) Oriented clay nanopaper from biobased components—mechanisms for superior fire protection properties. ACS Appl Mater Interfaces 7:5847–5856

Carosio F, Cuttica F, Medina L, Berglund LA (2016) Clay nanopaper as multifunctional brick and mortar fire protection coating—wood case study. Mater Des 93:357–363

Chen P, Cho SY, Jin H-J (2010) Modification and applications of bacterial celluloses in polymer science. Macromol Res 18:309–320

Cheng K-C, Catchmark JM, Demirci A (2009) Enhanced production of bacterial cellulose by using a biofilm reactor and its material property analysis. J Biol Eng 3:12. doi:10.1186/1754-1611-3-12

Eichhorn SJ, Dufresne A, Aranguren M, Marcovich NE, Capadona JR, Rowan SJ, Weder C, Thielemans W, Toman M, Renneckar S, Gindl W, Veigel S, Keckes J, Yano H, Abe K, Nogi M, Nakagaito AN, Mangalam A, Simonsen J, Benight AS, Bismarck A, Berglund LA, Peijs T (2010) Review: current international research into cellulose nanofibres and nanocomposites. J Mater Sci 45:1–33

Eronen P, Junka K, Laine J, Österberg M (2011) Interaction between water-soluble polysaccharides and native nanofibrillar cellulose thin films. BioResources 6:4200–4217

Gröndahl M, Eriksson L, Gatenholm P (2004) Material properties of plasticized hardwood xylans for potential application as oxygen barrier films. Biomacromolecules 5:1528–1535

Hansen NL, Blomfeldt TJ, Hedenqvist M, Plackett D (2012) Properties of plasticized composite films prepared from nanofibrillated cellulose and birch wood xylan. Cellulose 19:2015–2031

Henriksson M, Berglund LA (2007) Structure and properties of cellulose nanocomposite films containing melamine formaldehyde. J Appl Polym Sci 106:2817–2824

Henriksson M, Berglund LA, Isaksson P, Lindström T, Nishino T (2008) Cellulose nanopaper structures of high toughness. Biomacromolecules 9:1579–1585

Iwamoto S, Abe K, Yano H (2008) The effect of hemicelluloses on wood pulp nanofibrillation and nanofiber network characteristics. Biomacromolecules 9:1022–1026

Klemm D, Kramer F, Moritz S, Lindstroem T, Ankerfors M, Gray D, Dorris A (2011) Nanocelluloses: a new family of nature-based materials. Angew Chem Int Ed 50:5438–5466

Lee K-Y, Bismarck A (2012) Susceptibility of never-dried and freeze-dried bacterial cellulose towards esterification with organic acid. Cellulose 19:891–900

Lee K-Y, Blaker JJ, Bismarck A (2009) Surface functionalisation of bacterial cellulose as the route to produce green polylactide nanocomposites with improved properties. Compos Sci Technol 69:2724–2733

Lee K-Y, Bharadia P, Blaker JJ, Bismarck A (2012a) Short sisal fibre reinforced bacterial cellulose polylactide nanocomposites using hairy sisal fibres as reinforcement. Compos Part A Appl Sci 43:2065–2074

Lee K-Y, Ho KKC, Schlufter K, Bismarck A (2012b) Hierarchical composites reinforced with robust short sisal fibre preforms utilising bacterial cellulose as binder. Compos Sci Technol 72:1479–1486

Lee K-Y, Tammelin T, Schulfter K, Kiiskinen H, Samela J, Bismarck A (2012c) High performance cellulose nanocomposites: comparing the reinforcing ability of bacterial cellulose and nanofibrillated cellulose. ACS Appl Mater Interfaces 4:4078–4086

Lee K-Y, Aitomäki Y, Berglund LA, Oksman K, Bismarck A (2014a) On the use of nanocellulose as reinforcement in polymer matrix composites. Compos Sci Technol 105:15–27

Lee K-Y, Buldum G, Mantalaris A, Bismarck A (2014b) More than meets the eye in bacterial cellulose: biosynthesis, bioprocessing, and applications in advanced fiber composites. Macromol Biosci 14:10–32

Lee K-Y, Shamsuddin SR, Fortea-Verdejo M, Bismarck A (2014c) Manufacturing of robust natural fiber preforms utilizing bacterial cellulose as binder. J Vis Exp 1:e51432

Leppänen K, Spetz P, Pranovich A, Hartonen K, Kitunen V, Ilvesniemi H (2011) Pressurized hot water extraction of Norway spruce hemicelluloses using a flow-through system. Wood Sci Technol 45:223–236

Liu A, Berglund LA (2013) Fire-retardant and ductile clay nanopaper biocomposites based on montmorrilonite in matrix of cellulose nanofibers and carboxymethyl cellulose. Eur Polym J 49:940–949

Lozhechnikova A, Dax D, Vartiainen J, Willför S, Xu C, Österberg M (2014) Modification of nanofibrillated cellulose using amphiphilic block-structured galactoglucomannans. Carbohydr Polym 110:163–172

Lucenius J, Parikka K, Österberg M (2014) Nanocomposite films based on cellulose nanofibrils and water-soluble polysaccharides. React Funct Polym 85:167–174

Mariano M, El Kissi N, Dufresne A (2014) Cellulose nanocrystals and related nanocomposites: review of some properties and challenges. J Polym Sci Part B Polym Phys 52:791–806

Mautner A, Lee KY, Lahtinen P, Hakalahti M, Tammelin T, Li K, Bismarck A (2014) Nanopapers for organic solvent nanofiltration. Chem Commun 50:5778–5781

Mautner A, Lee K-Y, Tammelin T, Mathew AP, Nedoma AJ, Li K, Bismarck A (2015) Cellulose nanopapers as tight aqueous ultra-filtration membranes. React Funct Polym 86:209–214

Mikkonen K, Stevanic J, Joly C, Dole P, Pirkkalainen K, Serimaa R, Salmén L, Tenkanen M (2011) Composite films from spruce galactoglucomannans with microfibrillated spruce wood cellulose. Cellulose 18:713–726

Montrikittiphant T, Tang M, Lee K-Y, Williams CK, Bismarck A (2014) Bacterial cellulose nanopaper as reinforcement for polylactide composites: renewable thermoplastic nanopapreg. Macromol Rapid Commun 35:1640–1645

Moon RJ, Martini A, Nairn J, Simonsen J, Youngblood J (2011) Cellulose nanomaterials review: structure, properties and nanocomposites. Chem Soc Rev 40:3941–3994

Nakagaito AN, Yano H (2005) Novel high-strength biocomposites based on microfibrillated cellulose having nano-order-unit web-like network structure. Appl Phys A 80:155–159

Nogi M, Yano H (2008) Transparent nanocomposites based on cellulose produced by bacteria offer potential innovation in the electronics device industry. Adv Mater 20:1849–1852

Olszewska A, Junka K, Nordgren N, Laine J, Rutland MW, Österberg M (2013a) Non-ionic assembly of nanofibrillated cellulose and polyethylene glycol grafted carboxymethyl cellulose and the effect of aqueous lubrication in nanocomposite formation. Soft Matter 9:7448–7457

Olszewska A, Valle-Delgado JJ, Nikinmaa M, Laine J, Österberg M (2013b) Direct measurements of non-ionic attraction and nanoscaled lubrication in biomimetic composites from nanofibrillated cellulose and modified carboxymethylated cellulose. Nanoscale 5:11837–11844

Österberg M, Vartiainen J, Lucenius J, Hippi U, Seppälä J, Serimaa R, Laine J (2013) A fast method to produce strong NFC films as a platform for barrier and functional materials. ACS Appl Mater Interfaces 5:4640–4647

Paakko M, Vapaavuori J, Silvennoinen R, Kosonen H, Ankerfors M, Lindstrom T, Berglund LA, Ikkala O (2008) Long and entangled native cellulose I nanofibers allow flexible aerogels and hierarchically porous templates for functionalities. Soft Matter 4:2492–2499

Parikka K, Leppänen A-S, Pitkänen L, Reunanen M, Willför S, Tenkanen M (2010) Oxidation of polysaccharides by galactose oxidase. J Agric Food Chem 58:262–271

Peng X-W, Ren J-L, Zhong L-X, Sun R-C (2011) Nanocomposite films based on xylan-rich hemicelluloses and cellulose nanofibers with enhanced mechanical properties. Biomacromolecules 12:3321–3329

Pimenta S, Pinho ST (2011) Recycling carbon fibre reinforced polymers for structural applications: technology review and market outlook. Waste Manag (Oxford) 31:378–392

Pommet M, Juntaro J, Heng JYY, Mantalaris A, Lee AF, Wilson K, Kalinka G, Shaffer MSP, Bismarck A (2008) Surface modification of natural fibers using bacteria: depositing bacterial cellulose onto natural fibers to create hierarchical fiber reinforced nanocomposites. Biomacromolecules 9:1643–1651

Sehaqui H, Liu A, Zhou Q, Berglund LA (2010) Fast preparation procedure for large, flat cellulose and cellulose/inorganic nanopaper structures. Biomacromolecules 11:2195–2198

Sehaqui H, Ezekiel Mushi N, Morimune S, Salajkova M, Nishino T, Berglund LA (2012) Cellulose nanofiber orientation in nanopaper and nanocomposites by cold drawing. ACS Appl Mater Interfaces 4:1043–1049

Sehaqui H, Zhou Q, Berglund LA (2013) Nanofibrillated cellulose for enhancement of strength in high-density paper structures. Nord Pulp Pap Res J 28:182–189

Seifert M, Hesse S, Kabrelian V, Klemm D (2004) Controlling the water content of never dried and reswollen bacterial cellulose by the addition of water-soluble polymers to the culture medium. J Polym Sci Part A Polym Chem 42:463–470

Tomé L, Fernandes SM, Perez D, Sadocco P, Silvestre AD, Neto C, Marrucho I, Freire CR (2013) The role of nanocellulose fibers, starch and chitosan on multipolysaccharide based films. Cellulose 20:1807–1818

USDA (1970) Thermal degradation of wood components. U.S. Department of Agriculture, Forest Service, Forest Laboratory, Madison

Wan YZ, Hong L, Jia SR, Huang Y, Zhu Y, Wang YL, Jiang HJ (2006) Synthesis and characterization of hydroxyapatite–bacterial cellulose nanocomposites. Compos Sci Technol 66:1825–1832

Wang M, Olszewska A, Walther A, Malho J-M, Schacher FH, Ruokolainen J, Ankerfors M, Laine J, Berglund LA, Österberg M, Ikkala O (2011) Colloidal ionic assembly between anionic native cellulose nanofibrils and cationic block copolymer micelles into biomimetic nanocomposites. Biomacromolecules 12: 2074–2081

Wielinga WC (ed) (2009) Galactomannans. Handbook of hydrocolloids. Woodhead Publishing, Cambridge

Xu C, Willför S, Sundberg K, Petterson C, Holmbom B (2008) Physico-chemical characterization of spruce galactoglucomannan solutions: stability, surface activity and rheology. Cellul Chem Technol 41:51–62

Yano H, Sugiyama J, Nakagaito AN, Nogi M, Matsuura T, Hikita M, Handa K (2005) Optically transparent composites reinforced with networks of bacterial nanofibers. Adv Mater 17:153–155

Zhou Q, Malm E, Nilsson H, Larsson PT, Iversen T, Berglund LA, Bulone V (2009) Nanostructured biocomposites based on bacterial cellulosic nanofibers compartmentalized by a soft hydroxyethylcellulose matrix coating. Soft Matter 5:4124–4130